Contents lists available at ScienceDirect

Deep-Sea Research Part II

journal homepage: http://www.elsevier.com/locate/dsr2

Zooplankton community structure and dominant copepod population structure on the southern Kerguelen Plateau during summer 2016

Kohei Matsuno [a,b,c,*], Jake R. Wallis [c,d], So Kawaguchi [c,e], Sophie Bestley [d,f], Kerrie M. Swadling [c,d]

[a] Graduate School of Fisheries Sciences, Hokkaido University, 3-1-1 Minato-cho, Hakodate, Hokkaido, 041-8611, Japan
[b] Arctic Research Center, Hokkaido University, Kita-21 Nishi-11 Kita-ku, Sapporo, Hokkaido, 001-0021, Japan
[c] Antarctic Climate & Ecosystems Cooperative Research Centre, 20 Castray Esplanade, Battery Point, Tasmania, 7004, Australia
[d] Institute for Marine and Antarctic Studies, University of Tasmania, 20 Castray Esplanade, Battery Point, Tasmania, 7004, Australia
[e] Australian Antarctic Division, 203 Channel Highway, Kingston, Tasmania, 7050, Australia
[f] CSIRO Oceans and Atmosphere, GPO Box 1538, Hobart, Tasmania, 7001, Australia

A B S T R A C T

The influence of environmental factors on the horizontal community structure of zooplankton over the southern Kerguelen Plateau was investigated during summer in 2016. Zooplankton abundance ranged from 1490 to 363,484 ind. 1000 m^{-3}, with highest numbers observed in the eastern and central areas. Based on cluster analysis the zooplankton were divided into six groups (A–F), and these were only distinguished based on water masses and frontal systems. Groups A to C had abundant zooplankton and were consistent with areas of high chlorophyll *a* concentration. Group D represented low abundance near the southern Antarctic Circumpolar Current front, while group E was clustered south of the Southern Boundary and group F comprised two stations to the east of the Fawn Trough. Generalised linear model (GLM) highlighted both fronts and chlorophyll *a* concentration as drivers of overall zooplankton distribution. However, the population structures of key species were more likely a result of species-specific life cycles rather than water masses and frontal systems.

1. Introduction

The Kerguelen Plateau, and areas to the south, represents one of the most important regions for primary production in the Indian sector of the Southern Ocean (Arrigo et al., 2008), with high stocks of toothfish and krill found in the north and south, respectively (Duhamel et al., 2014; Nicol, 2006). However, the southern Kerguelen Plateau has never been investigated as a single region to determine the distribution and abundances of key species, their habitat characteristics, and the transition between the northern fish-based food web (Pruvost et al., 2005) and the southern krill-based food web (Nicol et al., 2012). Zooplankton play a key role in both food webs, as conduits for transferring energy from primary producers to higher trophic levels. To date, the zooplankton in the southern Kerguelen region have not been well described.

In the Southern Ocean, seawater temperature and variability in sea-ice extent are increasing (Bracegirdle et al., 2008; Turner et al., 2014), although the magnitude and direction of these changes differ among regions around Antarctica (Constable et al., 2014). Zooplankton

communities are influenced by the different frontal zones in the Southern Ocean (Errhif et al., 1997; Hunt and Hosie, 2005; Ward et al., 2012; Tachibana et al., 2017), and shifts in the fronts are expected to induce changes in zooplankton distributions (Constable et al., 2014). For example, a modelled 1 °C temperature rise produced a poleward shift for all zooplankton taxa (Atkinson et al., 2012). Food web structures are not well understood for the East Antarctic, compared to, for example, the Scotia Sea (Murphy et al., 2007), the Antarctic Peninsula (Ducklow et al., 2006) and the Ross Sea (Smith et al., 2007). Long-term programs such as the Southern Ocean CPR survey (McLeod et al., 2010) have provided information on the patterns of abundance and distribution of zooplankton for much of East Antarctica; however, they do not cover the southern Kerguelen Plateau, the focus of the current study.

The Kerguelen Plateau is an area of significant ecological value, with high krill biomass to the south (Pauly et al., 2000), and seabirds, seals and whales, using the plateau for migration and feeding (Patterson et al., 2016). The Kerguelen Axis (KAxis) voyage was designed as a synoptic survey, with multiple transects between 57.6 °S and 65.5 °S and 73.3°E

---

and 93.6 °E (Fig. 1). The transects encompassed an oceanographically complex region (Park et al., 2009), including the ice edge, the Southern Boundary (SB) of the Antarctic Circumpolar Current (ACC) and the Southern ACC Front (SAACF). The KAXIS research project aimed to identify and spatially distinguish krill-based and copepod-fish-based food webs and was designed to examine distribution of the food web components from bacteria to mid-trophic levels (fish and squid). This part of the program aimed to describe the horizontal distribution of zooplankton over the Southern Kerguelen Plateau. The population structures of dominant large (>2 mm) copepods are also presented. Finally, to evaluate the effects of environmental factors on zooplankton distribution, and to determine whether distinct communities were associated with large-scale oceanographic features we applied generalised linear modelling (GLM) and multivariate statistics. This approach has the potential to provide powerful insights into the influence of environmental factors on zooplankton distributions in the Southern Ocean, particularly environmentally variable regions such as the Kerguelen Plateau (Park et al., 2009).

2. Materials and methods

2.1. Field sampling

Thirty-seven sites were sampled over the southern Kerguelen Plateau, including the BANZARE Bank and the Princess Elizabeth Trough, from 23 January to 19 February 2016, onboard the *RSV Aurora Australis* (Fig. 1, Supplementary 1). At each site zooplankton were sampled using an RMT1+8 net, which was deployed by standard double oblique tows from the surface to 200 m. The RMT1 net had a mesh size of 315 μm and mouth area of 1 m². The towing speed of the RMT1+8 net ranged between 0.8 and 1.5 m s⁻¹ knots (mean = 1.1 m s⁻¹). A flow meter was positioned in the mouth of the RMT8 net to calculate the volume of water filtered; these values were divided by a factor of 9.42 to calculate the volume of water filtered by the RMT1, as per Ikeda et al. (1986). The RMT was fitted with hard cod ends to ensure that the organisms collected were in good condition. Upon retrieval, samples were immediately preserved in 4% buffered formaldehyde solution.

A SeaBird SBE911 plus CTD mounted on a SeaBird rosette sampler was deployed at each station to the full depth of the water column (see

Fig. 1. Sampling stations along the Kerguelen Axis in the Southern Ocean during January and February 2016.

Bestley et al., 2018 for details). Profiles of salinity, temperature and fluorescence were recorded at each station.

2.2. Samples and data analysis

In the laboratory, zooplankton samples were split with a Motoda box splitter so that a minimum of 550 individuals was enumerated per sample. Zooplankton were identified to species level where possible and counted under a stereomicroscope (Leica M165C). Large-sized copepods (adults >2 mm; i.e. *Calanoides acutus, Calanus propinquus, Calanus simillimus, Metridia gerlachei, Metrida lucens* and *Rhincalanus gigas*) were identified to copepodite stage. To identify the zooplankton, we referred to Razouls (1994) for copepods, Kirkwood (1982) for euphausiids, and Boltovskoy (1999) for other species. Abundance is reported as the number of individuals 1000 m⁻³.

The mean copepodid stage (*MCS*) of the six large copepods was calculated for each station where they occurred using the following equation:

$$MCS = \frac{\sum_{i=1}^{6} i \times Ai}{\sum_{i=1}^{6} Ai} \tag{1}$$

where i is the copepodite stage (1–6 indicates copepodid stage 1– copepodid stage 6), and Ai is the abundance (ind. 1000 m⁻³) of the ith copepodid stage (Marin, 1987).

Multivariate analyses, designed to explore relationships between zooplankton and their environment, were performed with PRIMER v7 (PRIMER-e). Abundance of each taxon was fourth-root transformed prior to cluster analysis to reduce the effect of abundant species (Quinn and Keough, 2002). A similarity matrix based on stations was constructed using the Bray-Curtis index, which is useful for biological data when there are many zeros (Quinn and Keough, 2002). For grouping the samples (Q-mode analysis), the similarity indices were coupled with hierarchical agglomerative clustering using a complete linkage method: Unweighted Pair Group Method using Arithmetic mean (UPGMA; Field et al., 1982). Accompanying this analysis, similarity profile analysis (SIMPROF) was added to determine if groupings of the stations were statistically significant (at 5% significance level). Similarity percentages (SIMPER) analysis was applied to determine which species contributed to the top 50% of total abundance for each group. Non-metric multi-dimensional scaling (NMDS) with multiple regression analysis was undertaken to explore relationships between the sampling sites and environmental data.

Regional differences in mean abundance among groups were tested by one-way ANOVA and the Tukey-Kramer post-hoc test was applied to distinguish which groups were statistically different. Additionally, a Mann-Whitney *U* test was performed on abundance between the clustering groups (A-C vs D-F) using R (version 3.4.0; R Core Team, 2017).

To find potential indicator species in the groups that resulted from the cluster analysis, the program Indicator Value (IndVal) was applied (Dufrêne and Legendre, 1997). IndVal was calculated as:

$$IndVal_{ij} = A_{ij} * B_{ij} * 100 \tag{2}$$

where A_{ij} = Nindividuals$_{ij}$/Nindividuals$_i$, and B_{ij} = Nsite$_{ij}$/Nsites$_j$. A_{ij} is a measure of site specificity, where Nindividuals$_{ij}$ is the mean number of individuals in species i across sites of group j, and Nindividuals$_i$ is the sum of the mean numbers of individuals of species i over all groups. B_{ij} is a measure of group fidelity, where Nsite$_{ij}$ is the number of sites in group j where species i is present, while Nsite$_j$ is the total number of sites in that group (Dufrêne and Legendre, 1997).

To evaluate the effects of environmental drivers on zooplankton community structure, we applied generalised linear models (GLMs, R version 3.4.0; R Core Team, 2017). To run the GLMs for each taxon we used a negative binominal distribution based on count data, with filtered volume applied as an offset. *MCS* of the copepods were tested based on the gaussian distribution. We tested for overdispersion by calculating
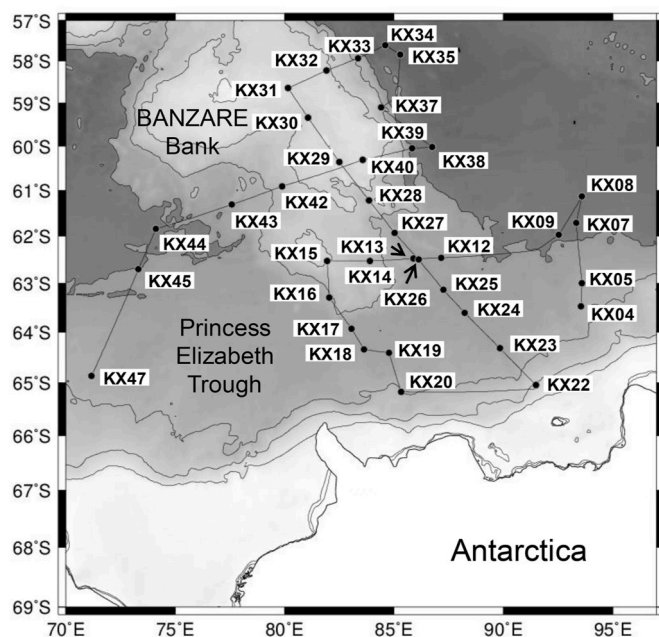
the dispersion parameter (Pearson's chi-square statistic/degrees of freedom in residual deviance) and found that values were close to 1 (0.89–1.34), indicating the models captured most of the variation. Only radiolarians had a dispersion parameter (1.89) that justified their removal from further GLM. The following factors were included in the GLM: depth (of the water column); chlorophyll *a* concentration (chl.*a*) as a measure of food availability; density averaged over the top 10 dbar, where low values can indicate recent sea ice melt; salinity$_{200}$, which has a direct effect on zooplankton physiology; MLD (mixed layer depth) as shallower depths can enhance primary production leading to more food for zooplankton; Temp$_{200}$, average temperature over the top 200 m as zooplankton metabolism is coupled tightly to temperature; time since melt, with the ice edge a region of high productivity and enhanced food supply; SST (sea surface temperature); and PAR (photosynthetically active radiation), as time when zooplankton are sampled can influence their position in the water column. Further details for defining each of these environmental variables are shown in Table 1. To remove multicollinearity among the environmental parameters we calculated variance inflation factors (VIF) for each parameter. If the VIF was higher than 3, it was removed from the explanatory parameters (O'Brien, 2007). To derive the final model, full models with all environmental variables were first constructed. Then, model selection was applied by "stepAIC" in the "MASS" package to choose the final models. Comparison between null and final models by ANOVA confirmed the goodness of fit of the model. If the *p* value < 0.05, then the final model was deemed to be better than the null model.

3. Results

3.1. Spatial changes in hydrographic condition

The surface mixed layer (SML) varied among stations, with the deepest at KX34 (68 m) and the shallowest at KX18-20 (13 m; Fig. 2a). Across the sampling region, the mean temperature of the upper 20 m of the water column (defined as SST) ranged from -1.68 to 3.75 °C; the

Table 1
Physical and biological variables included as predictors in the generalised linear models (GLMs). Oceanographic variables (temperature, salinity and density) were all derived from *in situ* CTD measurements undertaken at each RMT sampling site.

Variable	Explanation and source
Depth	Bathymetric depth (m) at sampling stations (Weatherall et al., 2015). Values are log10 transformed.
Chl.*a*	Integrated estimate of water column chlorophyll-*a* (mg m^{-2}; Westwood and Pearce, 2018) obtained using High Performance Liquid Chromatography following Wright et al. (2010), based on six CTD sampling depths within the upper 150 dbar.
Density	Mean potential density (kg m^{-3}) calculated relative to the surface (averaged over the upper 10 dbar). Low values (e.g. <26.8 kg m^{-3}) are indicative of recent ice influence/melt.
Salinity$_{200}$	Mean salinity over the depth between the surface and 200 m (the net sampling depth).
MLD	Mixed layer depth (m) estimates based on a change in density criterion of $\Delta\sigma\theta = 0.05$ kg m^{-3} relative to 10 dbar, following de Boyer Montégut et al. (2004).
Temp$_{200}$	Mean temperature over the depth between the surface and 200 m (the net sampling depth).
Time since melt	The time since ice melted (days) calculated from daily passive microwave estimates of sea ice concentration (%) obtained from the National Snow and Ice Data Center SMMR-SSM/I polar product available for the Southern Hemisphere gridded at 25 km resolution (Cavalieri et al., 1996, updated yearly; Maslanik and Stroeve, 1999, updated daily).
SST	Mean near-surface water temperature (°C, averaged over the upper 20 dbar).
PAR	Ship-based measurement of PAR (photosynthetically active radiation, Watts m^{-2}) averaged from the port and starboard underway data during the RMT sampling periods.

northeast area was warmest, while the southern area was cooler (Fig. 2b). The mean temperature averaged over the top 200 m of the water column (Fig. 2c) had a smaller range (-1.65° to 1.76 °C) compared with the top 20 m, while mean salinity in the top 200 m ranged from 34 to 34.48, with the northeast area being slightly fresher (Fig. 2d). Mean density in the upper SML ranged from 26.309 to 27.144 kg m^{-3}, indicting recent ice melt (Fig. 2e). Finally, Integrated chlorophyll *a* ranged from 19.7 to 132.8 mg m^{-2}, with stations KX04-KX09, KX39 and KX47 having concentrations higher than 100 mg m^{-2} (Fig. 2f).

3.2. Spatial changes in the zooplankton community

Total zooplankton abundance ranged from 1490 to 363,484 ind. 1000 m^{-3}, with the lowest abundance at KX43, and the largest at KX15 (Fig. 3a). Higher abundances were observed in the eastern and central areas. The zooplankton community was divided into 6 groups (A−F) at 75.7 and 78.7% similarity by Q-mode cluster analysis with SIMPROF, based on zooplankton abundances at each site (Fig. 4a). Based on one-way ANOVA and a Tukey-Kramer post-hoc test, the abundances of groups A and C were significantly higher than those of the remaining four groups (B, D-F; *p* < 0.0001). Additionally, the mean abundance of groups A-C was about 10 times higher than that of groups D-F (67,230 ± 79,473 vs 6193 ± 4035 ind. 1000 m^{-3}; Mann-Whitney *U* test, *p* < 0.01). Copepods were the dominant taxon in all six groups (59–76%), while foraminifera were the next most abundant group (4–31%; Fig. 4b). NMDS showed clear separation among the groups, with low stress (0.11). Five environmental factors, namely latitude, longitude, temperature, salinity and fluorescence, had correlations of $R^2 > 0.3$ with the groups based on associations among stations. The distribution of the groups across the sampling region broadly corresponded to water mass distribution (Fig. 5). Groups A, B and C were observed in the central and eastern areas, north of the subpolar zone and along the Kerguelen Plateau. Group D occurred in the central region, mainly in the northern part of the transect. Group E was observed from the Antarctic Slope Current to the Southern Boundary front, while Group F was in the Fawn Trough Current.

Based on the SIMPER analysis the copepods *Calanoides acutus*, *Calanus propinquus*, *Calanus simillimus*, *Ctenocalanus* spp., *Metridia gerlachei*, *Metridia lucens*, *Oithona* spp., *Oncaea* spp. and *Rhincalanus gigas,* the chaetognath *Eukrohnia hamata*, the euphausiid *Thysanoessa macrura*, radiolarians and foraminiferans were all important contributors to at least one group (Table 2). Foraminifera was the dominant taxon in four groups (A-D), while *C. acutus* was the second dominant species in groups A-C. *Oithona* spp. was the second dominant taxon in group D, and *M. gerlachei* was dominant in group E; *Ctenocalanus* spp. and *C. simillimus* were the dominant species in group F.

3.3. Spatial distribution of large-sized copepods

Calanoides acutus occurred at all stations along the transect, predominantly around the central region, with *MCS* values falling between CIII and CIV in the northwest and around CV towards the southeast (Fig. 6). *Calanus propinquus* also occurred at all stations, with younger copepodid stages more prevalent than for the *C. acutus* population (3.05 ± 0.54 vs 3.54 ± 0.72, Mann-Whitney *U* test, *p* < 0.01). *Calanus simillimus* were observed at only nine stations, most of them north of the Southern Boundary and mainly to the east of plateau; *MCS* was >4. *Metridia gerlachei* occurred at all stations and were abundant on the eastern-most transect and close to the continent; its average *MCS* was ∼ 4. *Metridia lucens* had a more northerly distribution than *M. gerlachei*, and its *MCS* ranged between 3.2 and 5. *Rhincalanus gigas* occurred at all stations, though in lower numbers than *C. acutus* and *C. propinquus* (728 ± 832 vs 6262 ± 12,834 and 2989 ± 4737 ind. 1000 m^{-3}, respectively). The mean *MCS* of *R. gigas* (4.5 ± 0.67) was higher than those of *C. acutus* and *C. propinquus*.
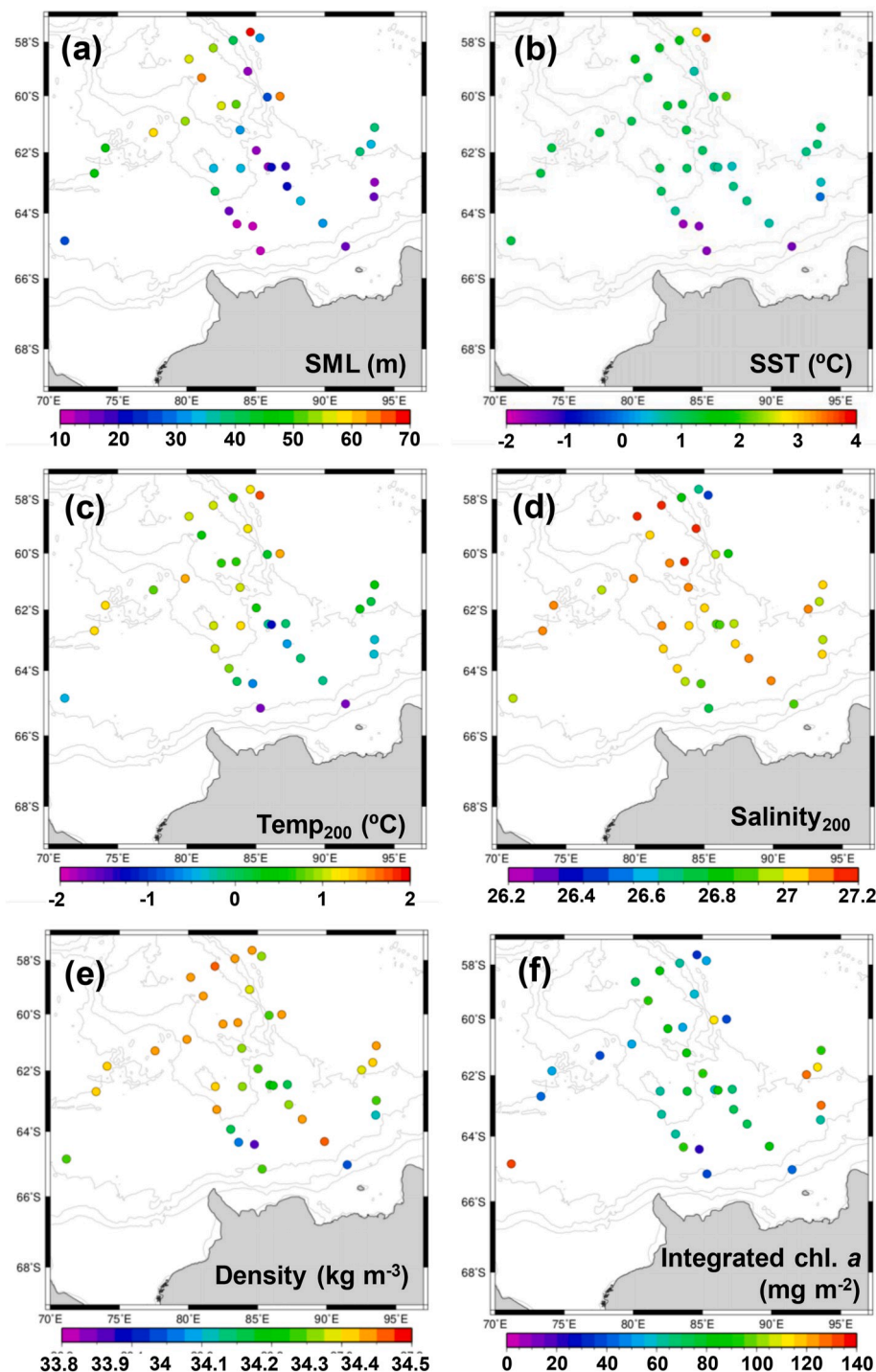
Fig. 2. Hydrographic conditions along the Kerguelen Axis. (a) depth of surface mixed layer (SML); (b) mean temperature in upper layer of SML averaged over the upper 20 dbar; (c) average temperature over the top 200 m; (d) average salinity over the top 200 m; (e) density averaged over the top 10 dbar: (f) chlorophyll *a* concentration averaged over the top 150 dbar.

3.4. Environmental drivers of the zooplankton community

Summaries of the results from the GLM are shown in Tables 3 and 4. For total zooplankton at each site, higher abundances were generally associated with warmer temperatures, higher chlorophyll *a*, shallower depths and decreased light intensity (night). When split into the main taxonomic groups, the effects of environmental drivers were similar to those shown for total zooplankton abundance. For euphausiacea, higher abundance was observed at stations where the mixed layer depths were shallow. The GLMs showed that abundances of five of the large-size (>2 mm) copepods (modelled separately), responded in a similar fashion to the total copepod group, although *M. gerlachei* showed higher abundances with cooler temperatures in the top 200 m of the water column. *Calanoides acutus* and *M. lucens* had increased abundance at stations where sea ice had persisted for longer.

For the mean copepodid stages of the large-sized copepods, the effects of environmental drivers varied with species. *Calanoides acutus* showed two positive (Density and Time since melt) and three negative relations ($Temp_{200}$, MLD, and chl.*a*), while *C. propinquus* exhibited one positive (Density) and two negative relationships ($Salinity_{200}$ and SST).
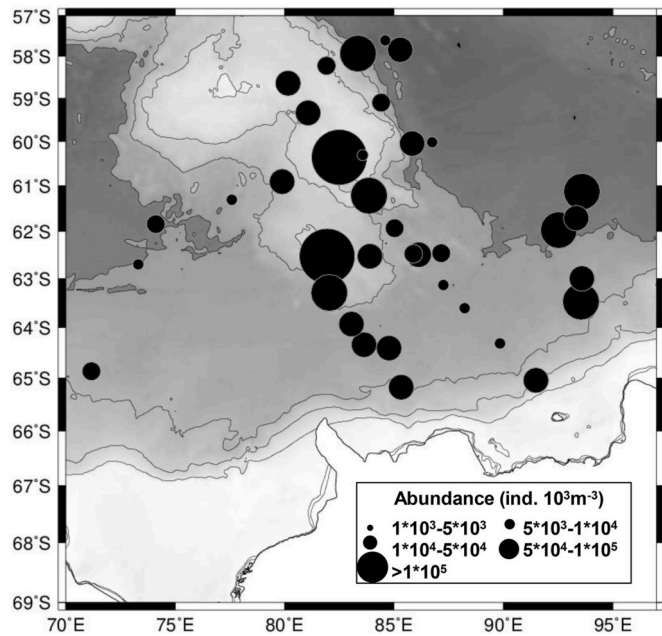
Fig. 3. Spatial distribution of total zooplankton abundance along the Kerguelen Axis during January and February 2016.

Metridia gerlachei had a weak positive relationship with $Temp_{200}$ and *M. lucens* had one positive (SST) and one negative (Depth). Younger stages in *R. gigas* occurred at stations were the MLD was shallower.

4. Discussion

4.1. Effects of water masses and frontal systems on zooplankton community

Studies of zooplankton on the southern Kerguelen Plateau are limited. Swadling et al. (2010) investigated the zooplankton community based on RMT1 samples to the region west (BROKE-West; 30–80°E) of the current study (71.2–93.6°E) during summer in 2006. In that survey, foraminifera, small copepods and appendicularians dominated the zooplankton community, while euphausiids (*Euphausia crystallorophias*) and the copepod *Metridia gerlachei* were highlighted as indicator species (Swadling et al., 2010). In the present study appendicularians were three orders of magnitude lower than observed in the BROKE-West study, while foraminiferans and radiolarians were much more abundant. Appendicularians have a short generation time (e.g. 8 day at 15 °C), which increases in colder temperatures (Deibel and Lowen, 2012). In polar regions, they can develop quickly and time their reproduction to the ice-edge phytoplankton bloom (Acuña et al., 1999); after reproduction, their abundance decreases rapidly following the end of the phytoplankton bloom. One hypothesis is that the lower numbers of appendicularians observed in the present study reflect some of the sites being sampled after the end of the phytoplankton bloom.

High numbers of foraminifera are found in the sea ice of the Southern Ocean, and are released into the water column with sea-ice melt (Ojima et al., 2017). This suggests foraminifera might be abundant where sea-ice cover persisted for the longest time and cells were released during the ice melt. Given that days after melt were generally lower than those recorded in Swadling et al. (2010), this might explain why the abundances recorded in the present study were up to 20 times higher than reported for BROKE-West. Despite this, we did not see a significant relationship between the ice-melt indices (i.e. Density and Time since melt) and abundance of foraminiferans. This might be explained by the fact that foraminifera are known to be influenced by many environmental factors, including snow depth and chl.*a* in the water column
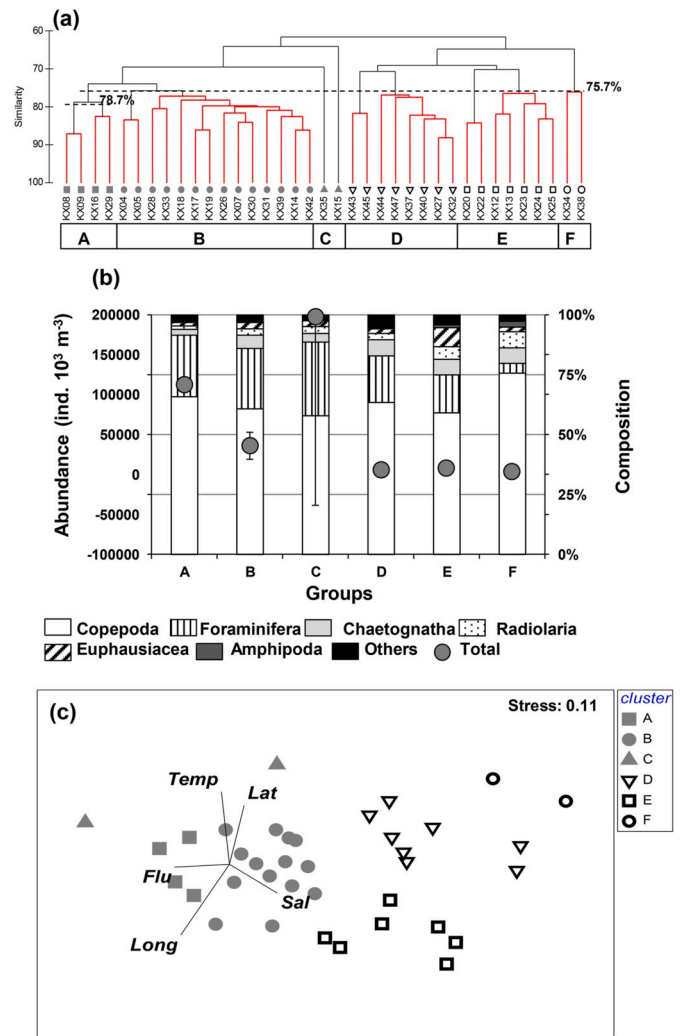

Fig. 4. (a) Results of Q-mode clustering based on abundance of zooplankton community. Red lines mean station groupings are not significant, as tested by SIMPROF. Labels show sampling stations. (b) Abundance and species composition of groups based on the cluster analysis at two similarity levels (from (a)). Error bars indicate standard deviation around total abundance of each group. (c) Non-metric multi-dimensional scaling (NMDS) plot with multiple regression analysis showing six groups based on the cluster analysis. Vectors show significant environmental factors. (For interpretation of the references to colour in this figure legend, the reader is referred to the Web version of this article.)

(Wallis et al., 2016). In our study, foraminifera were abundant in areas with high primary production, indicating that feeding preferences of foraminiferans might be an important driver.

The zooplankton communities found across the Southern Kerguelen Plateau in summer 2016 were split into two groups via multivariate analyses (groups A–C vs groups D–F) based on abundance. The distribution of the high-abundance group (i.e. groups A–C) was consistent with the distribution of high chl. *a*, highlighting possible foodweb interactions where the zooplankton were tracking the higher concentrations of phytoplankton. The GLM showed that total abundance of zooplankton was positively influenced by water-mass indices (i.e. $Temp_{200}$), lower light intensity (i.e. PAR) and increased phytoplankton biomasss (i.e. chl.*a*). The negative effect of light intensity on abundance suggested most species performed diel vertical migration during summer, whereby they were distributed deeper in the water column during the day (Takahashi et al., 2017). According to Swadling et al. (2010), the zooplankton community between 30 °E and 80 °E was correlated with chlorophyll *a* concentration, proximity to the Antarctic Slope Current
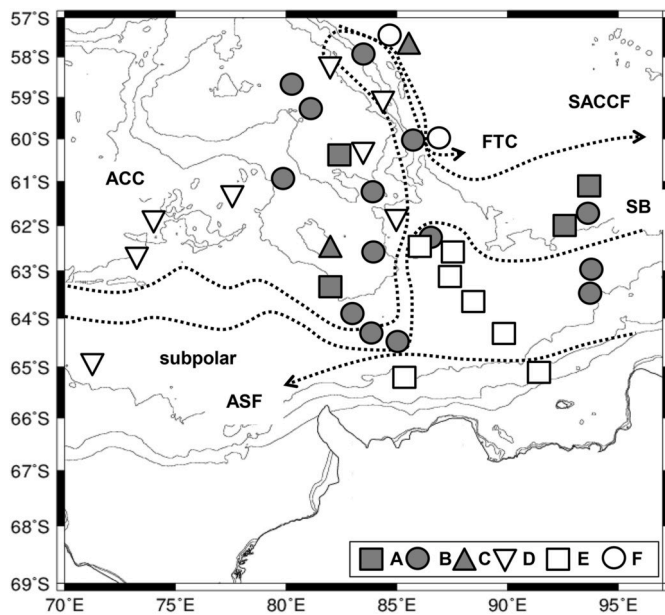
Fig. 5. Station groupings along the Kerguelen Axis, as determined from cluster analysis and NMDS. Positions of frontal systems based on Bestley et al. (2018). ACC: Antarctic Circumpolar Current; ASF: Antarctic Slope Front; FTC: Fawn Trough Current; SB: Southern Boundary; SACCF: Southern Antarctic Circumpolar Current Front.

and length of time without an ice cover. Thus, the zooplankton community across the western side of the Indian sector appears to be governed by the interplay of frontal systems, their vertical migration and bottom-up factors affecting productivity around the Kerguelen Plateau during summer.

Zooplankton assemblages are closely related to the different frontal zones in the Southern Ocean (Hunt and Hosie, 2005, 2006a, b; Hosie et al., 2014; Tachibana et al., 2017). Around the Kerguelen Plateau, several currents and frontal zones are observed (Park et al., 2009; Bestley et al., 2018). The ACC is disrupted by the plateau, which forces the core of the ACC to pass along its northern escarpment (e.g. Park et al., 1993). Following that, the southern Antarctic Circumpolar Current front (sAACf) and the Southern Boundary (SB) extend northward on the eastern edge of the Kerguelen Plateau. The Fawn Trough Current flows southeasterly at the northeast of the Kerguelen Plateau (Roquet et al., 2009). However, zonal homogeneity is broken by features such as gyres (Kaiser et al., 2009). These features of complicated oceanographic conditions potentially relate to zooplankton distribution. In this study the Southern Boundary clearly divided the zooplankton assemblages in the southeast region, while the central region was more homogeneous. This implies that a stable frontal system was present in the southeast region, with unstable system-induced gyres in the central region (Bestley et al., 2018).

4.2. Environmental drivers of zooplankton abundance and population structure of large-sized copepods

Population structure reflects growth and reproductive capacity and assists in our understanding of life cycles and the condition of a population (e.g. Atkinson, 1989). Mean copepodid stage (*MCS*) of copepods is a useful index for evaluating their population structure, with the value decreasing with input of new generations by reproduction and increasing with ontogenetic development within the population.

Calanoides acutus and *C. propinquus* are distributed widely in the Southern Ocean, from the Polar Front to the Antarctic coast; however, they are usually more abundant north of the SB-ACC and decrease towards the continent (e.g. Atkinson, 1996; Hosie et al., 2000; Tanimura

Table 2
Mean abundance (1000 m⁻³) for all species/taxon. **Bold** indicates IndVal of greater than 25% for that group. * represents top 50% of species in each group according to SIMPER analysis. Number in () represents N: number of sampling stations.

Species/taxon	Groups					
	A (4)	B (14)	C (2)	D (8)	E (7)	F (2)
Aetideopsis antarctica	0	1	0	0	1	0
Aetideopsis australis	0	0	**9**	0	0	0
Appendicularia	158	25	62	25	15	30
Calanoides acutus	**18223***	5836*	**34173***	607*	479	282*
Calanus nauplii	**1383**	109	444	164	7	0
Calanus propinquus	**6868***	3279*	**14628***	485*	468*	401*
Calanus simillimus	36	3	**1267**	0	0	**442***
Calanus spp. C1	**13345***	2895*	**16408**	468*	268	134*
Candacia sp.	**34**	0	9	0	0	1
Clausocalanus brevipes	**383**	205	**639**	37	38	13
Clausocalanus laticeps	62	26	9	5	0	**35**
Clio pyramidata forma sulcata	**223**	59	18	28	1	0
Clione limacina antarctica	0	**18**	0	1	4	0
Ctenocalanus spp.	**6847***	2165*	**6872***	285*	760*	458*
Cyllopus magellanicus	13	5	0	0	1	0
Euchirella rostromagna	**79**	24	9	5	5	1
Eukrohnia bathypelagica	0	5	**148**	1	0	0
Eukrohnia hamata	2690*	1809*	**6289***	355*	461*	186
Euphausia superba	0	32	**62**	1	21	0
Euphausia triacantha	0	0	**89**	0	0	0
Foraminifera	**28765***	9032*	60372	1072*	1255	124
Gaedius tenuispinus	13	7	0	2	4	0
Haloptilus longicirrus	**194**	41	0	2	6	2
Heterorhabdus austrinus	**353**	129	35	10	27	0
Hyperiella macronyx	88	9	**296**	6	0	42
Hyperiella sp.1(larva)	0	19	**148**	4	38	0
Isopoda	0	6	0	0	4	0
Limacina helicina	135	97	**157**	56	2	5
Limacina retroversa australis	0	0	18	1	0	**47**
Medusa	34	52	**157**	1	37	0
Metridia gerlachei	2523	1031	183	92	1088*	12
Metridia lucens	2831	627	**9925***	181	100	204*
Microcalanus pygmaeus	**237**	121	0	2	3	0
Oithona spp.	**10186***	1589*	**7458***	645*	276*	123*
Oncaea spp.	**3311***	1524*	**6621**	251*	308	81
Ostracoda	**809**	223	**1073**	54	139	3
Paraeuchaeta antarctica	**634**	166	**517**	17	168	6
Paraeuchaeta barbata	0	0	**9**	0	0	0
Pleuromamma robusta	57	7	**248**	9	5	0
Polychaeta	**1549**	406	**2070**	131	63	1
Primno macropa	72	**92**	44	5	43	1
Pseudochirella mawsoni	13	3	0	0	2	0
Racovitzanus antarcticus	554	147	**1931**	31	67	0
Radiolaria	1582	931*	**5293***	150	404*	209*
Rhincalanus gigas	**1714**	828	**2406***	104	378*	94
Rhincalanus gigas nauplii	2961*	776	**9352**	72	18	33
Sagitta gazellae	0	2	0	0	1	0
Sagitta marri	80	139	**349**	14	40	12
Sagitta maxima	0	13	**452**	0	5	3
Salp	**310**	82	**263**	11	53	0
Scaphocalanus farrani	**156**	35	18	4	3	0
Scaphocalanus vervoorti	**265**	28	0	0	29	0
Scina borealis	0	1	0	0	0	0
Scolecithricella minor	**642**	187	**946**	30	113	22
Scolecithricella ovata	**37**	4	0	0	0	0
Stephos longipes	**41**	12	0	1	0	1
Themisto gaudichaudii	**96**	10	18	4	20	26

(*continued on next page*)

Table 2 (*continued*)

Species/taxon	Groups					
	A (4)	B (14)	C (2)	D (8)	E (7)	F (2)
Thysanoessa macrura	1642	945	**4927**	103	600*	60
Undinella brevipes	**13**	0	0	0	0	0
Urchin larva	0	26	**444**	0	2	0
Vibilia antarctica	25	2	0	0	1	0
Vibilia armata	0	0	0	2	0	**5**
Total abundance	112264	35844	196864	5531	7832	3101

et al., 2008). In the present study, these two species were mainly found north of the Southern Boundary, and their population structures were similar in terms of abundance and *MCS*. Wallis et al. (2016) reported a positive influence on *C. propinquus* abundance from chl.*a* in water and sea ice, snow depth, latitude and year. In the present study, *C. propinquus* showed positive relationships with average temperature in the top 200 m and chlorophyll concentration, and negative relationships with average salinity, surface temperatures, water column depth and PAR. This species migrates into the surface layer in spring and reproduces, before descending into the deep layer for diapause during autumn (Schnack-Schiel et al., 1991; Atkinson, 1996). While the environmental drivers of abundances of *C. acutus* and *C. propinquus* were similar, the sea-ice melt indices (Density and Time since melt) showed negative relationships only with *C. acutus* abundances and positive relationships with their *MCS*. Thus, higher abundance of the younger stages was associated with lower surface density, suggesting a shorter time since sea-ice melt. *Calanoides acutus* reproduces from November to March in the Weddell Sea (Hagen and Schnack-Schiel, 1996), and the appearance of the cohort likely coincides with the high chlorophyll *a* concentration in the summer period (Atkinson, 1998). *Calanus simillimus* occurred in the northeast regions, particularly near the Fawn Trough Current. This species might have been transported south from more northerly warmer waters, because it is known to be distributed in subantarctic waters and northern parts of the ACC (Atkinson, 1998).

The two species of *Metridia* had different distributions: *M. gerlachei* was dominant in the south, while *M. lucens* had higher abundances in the north, a common pattern in the Southern Ocean (e.g. Atkinson, 1989). The GLM results indicated that abundance of *M. gerlachei* showed similar responses to those of *C. propinquus*, except for the effects of temperature: higher temperatures in the lower mixed layer resulted in higher abundance of *C. propinquus* and lower abundance of *M. gerlachei*. Light intensity did not have a strong influence on *Metridia* species compared to the other copepods. This was interesting because this genus is known to
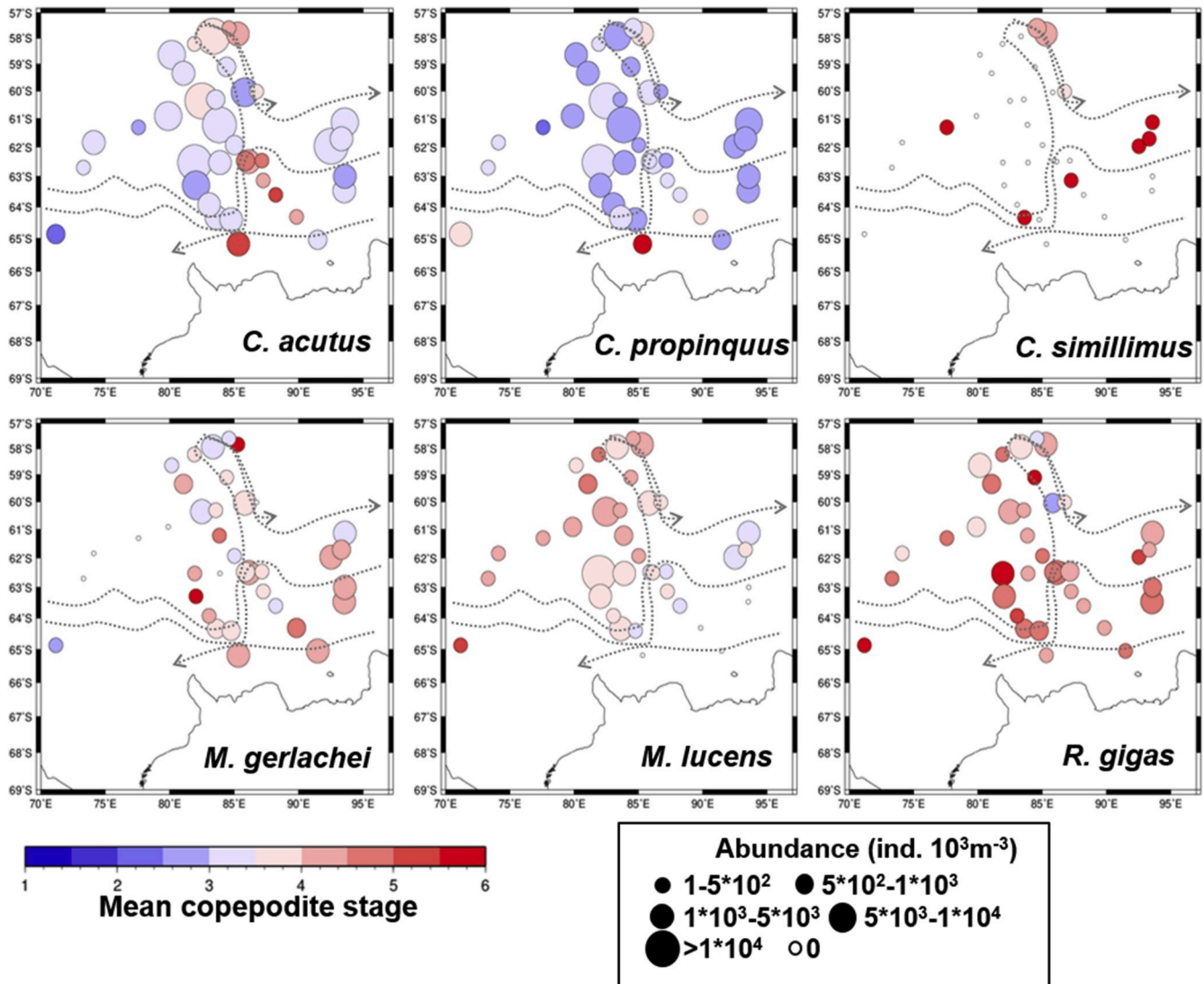

Fig. 6. Spatial distribution of dominant copepods along the Kerguelen Axis. Circle size and colour denotes the abundance and mean copepodite stage of each species. (For interpretation of the references to colour in this figure legend, the reader is referred to the Web version of this article.)

Table 3
Result of GLM and "stepAIC" analysis for zooplankton abundance and mean copepodid stage along the Kerguelen Axis transect. If a variable is included in the model for a taxon it is shown as positive (up arrow) when higher abundances are associated with higher values of the variable and negative (down arrow) when higher abundances are associated with lower values of the variable. Int.: intercept, remaining variables as per Table 1. If a variable is included in the model for a taxon it is shown with an arrow -: p *: $p < 0.05$; **: $p < 0.01$; ***: $p < 0.001$. MCS – mean copepodite stage.

	Intercept	Density	Salinity$_{200}$	SST	Temp$_{200}$	MLD	Depth	Chl.a	PAR	Time since melt	p value (ANOVA, null vs final)
Total zooplankton	***↑		***↓	***↓	***↑		***↓	***↑	**↓		***
Amphipoda								*↑			0.0605
Chaetognatha	***↑	***↓			**↑		**↓	***↑	**↓		**
Copepoda	***↑		***↓	***↓	***↑		***↓	***↑	**↓		***
Euphausiacea	*↑					*↓	*↓	-↓			*
Foraminifera	***↑		***↓	***↓	***↑		***↓	***↑	**↓		***
Copepods											
C. acutus	***↑	*↓	**↓		***↑		***↓	***↑	***↓	*↓	***
C. propinquus	***↑		***↓	**↓	***↑		***↓	***↑	***↓		***
M. gerlachei	**↑		**↓		***↓		-↓	***↑	*↓		***
M. lucens	**↑		**↓		***↑		**↓	**↑		*↓	***
R. gigas	**↑	*↓			-↑		*↓	*↑	**↓		*
Mean copepodite stage											
MCS_*C. acutus*	**↓	***↑			**↓	**↓		***↓		*↑	***
MCS_*C. propinquus*	*↑	***↑	***↓	***↓		-↓	-↓				***
MCS_*M. gerlachei*					-↑						0.3302
MCS_*M. lucens*	***↑			**↑			**↓				***
MCS_*R. gigas*	**↑					**↓	-↓		-↑		**

Table 4
Summary of the important environmental dependencies evident in the models.

Model	Features
Total zooplankton abundance	Generally, higher abundances were associated with warmer temperatures, higher chlorophyll-*a* concentration and shallower depth, which was consistent with high abundances observed over the southern Kerguelen plateau (Fig. 3). Lower abundances were associated with increased daylight.
Taxon abundances	Relationships mainly consistent with those reported for total zooplankton abundance. Additionally, chaetognaths were associated with surface low-Density. Higher abundances of euphausiids were associated with shallower mixed layer depths.
Large copepods	Relationships mainly consistent with those reported for total zooplankton abundance. However, *M. gerlachei* showed an opposite relation with temperature below the MLD. *C. acutus* and *M. lucens* were more abundant when there was a shorter time since sea-ice melt.
Copepod stages	The relationships varied with species.

comparing the environmental drivers of developmental stages of copepods using GLM. Thus, GLM is a powerful analytical tool capable of distinguishing structure within copepod populations even within complex oceanographic regions such as the south Kerguelen Plateau. Also, GLM helped determine those conditions that are most suited to each taxonomic assemblage. This information is useful for identifying productive regions and understanding the response of zooplankton to environmental change. In future, detailed information (e.g. population structure) for the main zooplankton species should be monitored and used in assessing the influence of climate change on key zooplankton species.

CRediT authorship contribution statement

Kohei Matsuno: Investigation, Formal analysis, Visualization, Writing - original draft. **Jake R. Wallis:** Methodology, Investigation. **So Kawaguchi:** Conceptualization, Investigation, Supervision. **Sophie Bestley:** Software, Validation. **Kerrie M. Swadling:** Conceptualization, Writing - review & editing, Supervision.

Acknowledgements

Appendix A. Supplementary data

Supplementary data to this article can be found online at https://doi.org/10.1016/j.dsr2.2020.104788.

undertake diel vertical migration rather than seasonal vertical migration (Atkinson and Peck, 1988; Huntley and Escritor, 1992; Schnack-Schiel and Hagen, 1995). The *MCS* for the two *Metridia* species were high and might not relate directly to chlorophyll distribution because these species have a long reproductive period (i.e. there is no clear reproductive-peak season) and distribute rather patchily without any apparent link to the distribution of chlorophyll (Atkinson, 1989, 1998). For *Rhincalanus gigas*, late copepodid stages were dominant, although their nauplii were observed in almost all samples (data not shown). The reproduction of this species is reported to occur mainly during summer (Atkinson, 1998), though with regional differences; e.g. reproduction continues into late autumn around the Antarctic Peninsula (Martin and Schnack-Schiel, 1993). *Rhincalanus gigas* was reproducing during the January and February in the Indian sector. From the GLM, the relationships of *R. gigas* with environmental drivers was similar to the other copepods, although chlorophyll *a* concentration was not a strong influence on this species.

Recently, research investigating environmental drivers of zooplankton abundance in the Southern Ocean via statistical modelling (e.g. GLM, generalised additive models) has increased (e.g. Wallis et al., 2016; Kelly et al., this issue), but studies using aspects of population structure (e.g. *MCS*) as a response variable in GLM are limited. In this study, the discussion of population structure was augmented by

References

Acuña, J.L., Deibel, D., Bochdansky, A.B., Hatfield, E., 1999. *In situ* ingestion rates of appendicularian tunicates in the northeast water Polynya (NE Greenland). Mar. Ecol. Prog. Ser. 186, 149–160.

Arrigo, K.R., Van Dijken, G.L., Bushinsky, S., 2008. Primary production in the Southern Ocean, 1997–2006. J. Geophys. Res. 113, C08004.

Atkinson, A., 1989. Distribution of six major copepod species around South Georgia in early summer. Polar Biol. 9, 353–363.

Atkinson, A., 1996. Subantarctic copepods in an oceanic, low chlorophyll environment: ciliate predation, food selectivity and impact on prey populations. Mar. Ecol. Prog. Ser. 130, 85–96.

Atkinson, A., 1998. Life cycle strategies of epipelagic copepods in the Southern Ocean. J. Mar. Syst. 15, 289–311.

Atkinson, A., Peck, J.M., 1988. A summer-winter comparison of zooplankton in the oceanic area around South Georgia. Polar Biol. 8, 463–473.

Atkinson, A., Ward, P., Hunt, B.P.V., Pakhomov, E.A., Hosie, G.W., 2012. An overview of Southern Ocean zooplankton data: abundance, biomass, feeding and functional relationships. CCAMLR Sci. 19, 171–218.

Bestley, S., van Wijk, E., Rosenberg, M., Eriksen, R., Corney, S., Tattersall, K., Rintoul, S., 2018. Ocean circulation and frontal structure near the southern Kerguelen Plateau: the physical context for the Kerguelen Axis ecosystem study. Deep-Sea Res. II. https://doi.org/10.1016/j.dsr1012.2018.1007.1013.

Boltovskoy, D. (Ed.), 1999. South Atlantic Zooplankton Volumes 1 & 2. Backhuys, Leiden.

Bracegirdle, T.J., Connolley, W.M., Turner, J., 2008. Antarctic climate change over the twenty-first century. J. Geophys. Res. 113, D03103.

Cavalieri, D.J., Parkinson, C.L., Gloersen, P., Zwally, H.J., 1996. Sea Ice Concentrations from Nimbus-7 SMMR and DMSP SSM/I-SSMIS Passive Microwave Data. updated yearly.. NASA National Snow and Ice Data Center Distributed Active Archive Center, Boulder, Colorado USA. Version 1. [January - February 1997 - 2015].

Constable, A.J., Melbourne-Thomas, J., Corney, S.P., Arrigo, K.R., Barbraud, C., Barnes, D.K., Bindoff, N.L., et al., 2014. Climate change and Southern Ocean ecosystems I: how changes in physical habitats directly affect marine biota. Global Change Biol. 20, 3004–3025.

de Boyer Montégut, C., Madec, G., Fischer, A.S., Lazar, A., Iudicone, D., 2004. Mixed layer depth over the global ocean: an examination of profile data and a profile-based climatology. J. Geophys. Res. 109, C12003.

Deibel, D., Lowen, B., 2012. A review of the life cycles and life-history adaptations of pelagic tunicates to environmental conditions. ICES J. Mar. Sci. 69, 358–369.

Ducklow, H.W., Fraser, W., Karl, D.M., Quetin, L.B., Ross, R.M., Smith, R.C., Stammerjohn, S.E., Vernet, M., Daniels, R.M., 2006. Water-column processes in the west antarctic Peninsula and the Ross Sea: interannual variations and foodweb structure. Deep-Sea Res. Part II 53, 834–852.

Dufrêne, M., Legendre, P., 1997. Species assemblages and indicator species: the need for a flexible asymmetrical approach. Ecol. Monogr. 67, 345–366.

Duhamel, G., Hulley, P.-A., Causse, R., Koubbi, P., Vacchi, M., Pruvost, P., Vigetta, S., Irisson, J.-O., Mormède, S., Belchier, M., Dettai, A., Detrich, H.W., Gutt, J., Jones, C. D., Kock, K.-H., Lopez, Abellan, L.J., Van de Putte, A.P., 2014. Chapter 7. Biogeographic patterns of fish. In: De Broyer, C., Koubbi, P., Griffiths, H.J., Raymond, B., d', Udekem d'Acoz C., Van de Putte, A.P., Danis, B., David, B., Grant, S., Gutt, J., Held, C., Hosie, G., Huettmann, F., Post, A., Ropert-Coudert, Y. (Eds.), Biogeographic Atlas of the Southern Ocean. Scientific Committee on Antarctic Research, Cambridge, pp. 328–362.

Errhif, A., Razouls, C., Mayzaud, P., 1997. Composition and community structure of pelagic copepods in the Indian sector of the Antarctic Ocean during the end of the austral summer. Polar Biol. 17, 418–430.

Field, J.G., Clarke, K.R., Warwick, R.M., 1982. A practical strategy for analyzing multispecies distribution patterns. Mar. Ecol. Prog. Ser. 8, 37–52.

Hagen, W., Schnack-Schiel, S.B., 1996. Seasonal lipid dynamics in dominant Antarctic copepods: energy for overwintering or reproduction? Deep-Sea Res. I 43, 139–158.

Hosie, G.W., Schultz, M.B., Kitchener, J.A., Cochran, T.G., Richards, K., 2000. Macrozooplankton community structure off East Antarctica (80−150°E) during the Austral summer of 1995/1996. Deep-Sea Res. II 47, 2437–2463.

Hosie, G., Mormède, S., Kitchener, J., Takahashi, K., Raymond, B., 2014. 10.3. Near-surface zooplankton communities. In: De Broyer, C., Koubbi, P., Griffiths, H.J., Raymond, B., d', Udekem d'Acoz C., Van de Putte, A.P., Danis, B., David, B., Grant, S., Gutt, J., Held, C., Hosie, G., Huettmann, F., Post, A., Ropert-Coudert, Y. (Eds.), Biogeographic Atlas of the Southern Ocean. Scientific Committee on Antarctic Research, Cambridge, pp. 422–430.

Hunt, B., Hosie, G., 2005. Zonal structure of zooplankton communities in the Southern Ocean South of Australia: results from a 2150 km continuous plankton recorder transect. Deep-Sea Res. I 52, 1241–1271.

Hunt, B., Hosie, G., 2006a. The seasonal succession of zooplankton in the Southern Ocean south of Australia, part I: the seasonal ice zone. Deep Sea Res. I 53, 1182–1202.

Hunt, B., Hosie, G., 2006b. The seasonal succession of zooplankton in the Southern Ocean south of Australia, part II: the sub-antarctic to Polar Frontal Zones. Deep Sea Res. I 53, 1203–1223.

Huntley, M.E., Escritor, F., 1992. Ecology of *Metridia gerlachei* Giesbrecht in the western Bransfield strait, Antarctica. Deep-Sea Res. 39, 1027–1055.

Ikeda, T., Hosie, G., Stolp, M., 1986. SIBEXII cruise krill/zooplankton data. ANARE (Aust. Natl. Antarct. Res. Exped.) Res. Notes. 32, 1–70.

Kaiser, S., Barnes, D.K.A., Sands, C.J., Brandt, A., 2009. Biodiversity of an unknown Antarctic Sea: assessing isopod richness and abundance in the first benthic survey of the Amundsen continental shelf. Mar. Biodivers. 39, 27. https://doi.org/10.1007/s12526-009-0004-9.

Kelly, P., Corney, S.P., Melbourne-Thomas, J., Kawaguchi, S., Bestley, S., Fraser, A., Swadling, K.M., This issue, Salpa thompsoni in the Indian Sector of the Southern Ocean: environmental drivers and life history parameters. Deep-Sea Res. II.

Kirkwood, J.M., 1982. A Guide to the Euphausiacea of the Southern Ocean (No. 1-5). Information Services Section, Antarctic Division, Dept. of Science and Technology.

Marin, V., 1987. The oceanographic structure of eastern Scotia Sea-IV. Distribution of copepod species in relation to hydrography in 1981. Deep-Sea Res. 34, 105–121.

Martin, V.H., Schnack-Schiel, S.B., 1993. The occurrence of *Rhincalanus gigas, Calanoides acutus*, and *Calanus propinquus* (Copepoda: Calanoida) in late May in the area of the antarctic Peninsula. Polar Biol. 13, 35–40.

Maslanik, J., Stroeve, J., 1999. DMSP SSMIS Daily Polar Gridded Sea Ice Concentrations. updated daily. Near-Real-Time. NASA National Snow and Ice Data Center Distributed Active Archive Center, Boulder, Colorado USA. Version 1. [January - February 2016]. Boulder, Colorado USA.

McLeod, D.J., Hosie, G.W., Kitchener, J.A., Takahashi, K.T., Hunt, B.P.V., 2010. Zooplankton atlas of the Southern Ocean: the SCAR SO-CPR survey (1991–2008). Pol. Sci. 4, 353–385.

Murphy, E.J., Watkins, J.L., Trathan, P.N., Reid, K., Meredith, M.P., Thorpe, S.E., Johnston, N.M., Clarke, A., Tarling, G.A., Collins, M.A., Forcada, J., Shreeve, R.S., Atkinson, A., Korb, R., Whitehouse, M.J., Ward, P., Rodhouse, P.G., Enderlein, P., Hirst, A.G., Martin, A.R., Hill, S.L., Staniland, I.J., Pond, D.W., Briggs, D.R., Cunningham, N.J., Fleming, A.H., 2007. Spatial and temporal operation of the Scotia Sea ecosystem: a review of large-scale links in a krill centred food web. Phil. Trans. Royal Soc. London Series B 362, 113–148.

Nicol, S., 2006. Krill, currents, and sea ice: *Euphausia superba* and its changing environment. Bioscience 56, 111–120.

Nicol, S., Foster, J., Kawaguchi, S., 2012. The fishery for Antarctic krill – recent developments. Fish Fish. 13, 30–40.

O'Brien, R.M., 2007. A caution regarding rules of thumb for variance inflation factors. Qual. Quantity 41, 673–690.

Ojima, M., Takahashi, K.T., Iida, T., Moteki, M., Miyazaki, N., Tanimura, A., Odate, T., 2017. Variability of the fauna within drifting sea ice floes in the seasonal ice zone of the Southern Ocean during the austral summer. Pol. Sci. 12, 19–24.

Park, Y.-H., Gambéroni, L., Charriaud, E., 1993. Frontal structure, water masses and circulation in the Crozet Basin. J. Geophys. Res. 98, 12361–12385. https://doi.org/10.1029/93JC00938.

Park, Y.-H., Vivier, F., Roquet, F., Kestenare, E., 2009. Direct observations of the ACC transport across the Kerguelen Plateau. Geophys. Res. Lett. 36, L18603. https://doi.org/10.1029/2009GL039617.

Patterson, T.A., Sharples, R.J., Raymond, B., Welsford, D.C., Andrews-Goff, V., Lea, M.A., Goldsworthy, S.D., Gales, N.J., Hindell, M., 2016. Foraging distribution overlap and marine reserve usage amongst sub-Antarctic predators inferred from a multi-species satellite tagging experiment. Ecol. Indicat. 70, 531–544.

Pauly, T., Nicol, S., Higginbottom, I., Hosie, G., Kitchener, J., 2000. Distribution and abundance of antarctic krill (*Euphausia superba*) off east Antarctica (80–150 E) during the austral summer of 1995/1996. Deep-Sea Res. II 47, 2465–2488.

Pruvost, P., Duhamel, G., Palomares, M.L.D., 2005. An ecosystem model of the Kerguelen Islands' EEZ. In: Palomares, M.L.D., Pruvost, P., Pitcher, T.J., Pauly, D. (Eds.), Modeling Antarctic Marine Ecosystems. Fisheries Centre Research Reports 13 (7. Fisheries Centre, University of British Columbia, Vancouver, Canada, pp. 40–64.

Quinn, G.P., Keough, M.J., 2002. Experimental Design and Data Analysis for Biologists. Cambridge University Press, Cambridge.

R Core Team, 2017. R: A Language and Environment for Statistical Computing. R Foundation for Statistical Computing, Vienna, Austria.

Razouls, C., 1994. Manuel d'identification des principals espèces de copépods pélagiques antarctiques et subantarctiques. Ann. Inst. Oceanogr. 70, 1–204.

Roquet, F., Park, Y.-H., Guinet, C., Bailleul, F., Charrassin, J.-B., 2009. Observations of the Fawn Trough current over the Kerguelen Plateau from instrumented elephant seals. J. Mar. Syst. 78, 377–393.

Schnack-Schiel, S.B., Hagen, W., 1995. Life-cycle strategies of *Calanoides acutus, Calanus propinquus*, and *Metridia gerlachei* Copepoda: Calanoida in the eastern Weddell Sea, Antarctica. ICES J. Mar. Sci. 52, 541–548.

Schnack-Schiel, S.B., Hagen, W., Mizdalski, E., 1991. Seasonal comparison of *Calanoides acutus* and *Calanus propinquus* (Copepoda: Calanoida) in the southeastern Weddell Sea, Antarctica. Mar. Ecol. Prog. Ser. 70, 17–27.

Smith Jr., W.O., Ainley, D.G., Cattaneo-Vietti, R., 2007. Trophic interactions within the Ross Sea continental shelf ecosystem. Phil. Trans. Royal Soc. London Series B 362, 95–111.

Swadling, K.M., Kawaguchi, S., Hosie, G.W., 2010. Antarctic mesozooplankton community structure during BROKE-West (30°E−80°E), January–February 2006. Deep-Sea Res. II 57, 887–904.

Tachibana, A., Watanabe, Y., Moteki, M., Hosie, G.W., Ishimaru, T., 2017. Community structure of copepods in the oceanic and neritic waters off Adélie and George V Land, East Antarctica, during the austral summer of 2008. Pol. Sci. 12, 34–45.

Takahashi, K.T., Hosie, G.W., Odate, T., 2017. Intra-annual seasonal variability of surface zooplankton distribution patterns along a 110°E transect of the Southern Ocean in the austral summer of 2011/12. Pol. Sci. 12, 46–58.

Tanimura, A., Kawaguchi, S., Oka, N., Nishikawa, J., Toczko, S., Takahashi, K.T., Terazaki, M., Odate, T., Fukuchi, M., Hosie, G., 2008. Abundance and grazing impacts of krill, salps and copepods along the 140°E meridian in the Southern Ocean during summer. Antarct. Sci. 20, 365–379.

Turner, J.A., Barrand, N.E., Bracegirdle, T.J., Convey, P., Hodgson, D.A., Jarvis, M., Jenkins, A., Marshall, G., Meredith, M.P., Roscoe, H., Shanklin, J., 2014. Antarctic climate change and the environment: an update. Polar Rec. 50, 237–259.

Wallis, J.R., Swadling, K.M., Everett, J.D., Suthers, I.M., Jones, H.J., Buchanan, P.J., Crawford, C.M., James, L.C., Johnson, R., Meiners, K.M., Virtue, P., Westwood, K., Kawaguchi, S., 2016. Zooplankton abundance and biomass size spectra in the East Antarctic sea-ice zone during the winter–spring transition. Deep-Sea Res. II 131, 170–181.

Ward, P., Atkinson, A., Venables, H.J., Tarling, G.A., Whitehouse, M.J., Fielding, S., Collins, M.A., Korb, R., Black, A., Stowasser, G., Schmidt, K., Thorpe, S.E., Enderlein, P., 2012. Food web structure and bioregions in the Scotia Sea: a seasonal synthesis. Deep-Sea Res. II 59, 253–266.

Weatherall, P., Marks, K.M., Jakobsson, M., Schmitt, T., Tani, S., Arndt, J.E., Rovere, M., Chayes, D., Ferrini, V., Wigley, R., 2015. A new digital bathymetric model of the world's oceans. Earth Space Sci. 2, 331–345.

Westwood, K., Pearce, I., 2018. Chlorophyll K-Axis Voyage V3 2015/16. Australian Antarctic Data Centre. https://doi.org/10.4225/15/5a94c701b98a8.

Wright, S.W., van den Enden, R.L., Pearce, I., Davidson, A.T., Scott, F.J., Westwood, K.J., 2010. Phytoplankton community structure and stocks in the Southern Ocean (30–80°E) determined by CHEMTAX analysis of HPLC pigment signatures. Deep-Sea Res. II 57, 758–778.